Environmental Science
Processes & Impacts

PAPER

Cite this: *Environ. Sci.: Processes Impacts*, 2014, **16**, 1772

Practical strategies for identifying groundwater discharges into sediment and surface water with fiber optic temperature measurement

John Selker,[a] Frank Selker,[a] Julie Huff,[a] Russ Short,[b] Deborah Edwards,[c] Peter Nicholson[c] and Arthur Chin[c]

Received 23rd December 2013
Accepted 29th April 2014

DOI: 10.1039/c3em00716b

rsc.li/process-impacts

Identifying or ruling out groundwater discharges into sediment and surface waters is often critical for evaluating impacts and for planning remedial actions. Information about subsurface structure and groundwater can be helpful, but imperfect information, heterogeneous materials, and the likelihood of preferential pathways make it difficult to locate seeps without direct seep monitoring. We present the practical application of a method that uses fiber optic temperature measurement to provide high-resolution, sensitive, and dynamic monitoring of seepage from sediments over large areas: distributed temperature sensing to identify groundwater discharge (DTSID). First, we introduce a stochastic Monte Carlo method for designing DTSID installation based on site characteristics and the required probability of detecting particular size seeps. We then present practical methods for analysing DTSID results to prioritize locations for further investigation used at three industrial locations. Summer conditions generally presented greater difficulty in the method due to stronger environmentally-driven temperature fluctuations and thermal stratification of surface water. Tidal fluctuations were shown to be helpful in seepage detection at some locations by creating a dynamic temperature pattern that likely reflects changing seepage with varying water levels. At locations with suitable conditions for the application of DTSID, it can provide unique information regarding likely seep locations, enhancing an integrated site investigation.

Environmental impact

This work provides immediate insight to environmental processes and impacts by providing a validated approach to identification of the location of points of entry of potentially contaminated groundwater into surface water receiving bodies. In the past these seeps have been invisible, and thus remediation has been ill-focused with respect to the true location and magnitude of potential contaminant pathways. The manuscript presents a practicable design and implementation of a method to locate seeps of any specified size. These can then be subject to strategic monitoring, and thereby focusing remedial efforts on actual problems. This approach may well become an industry norm in such settings, as demonstrated by the wide range of sites presented in this paper.

Introduction

A fundamental challenge of addressing contaminated sites near bodies of water is the identification of points of discharge of contaminated groundwater into sediment and surface water. An equally important need is confidence regarding the absence of seeps in other areas. This second question, essential to cost effective remediation, bedevils discrete sampling methods: how do we know that sampling didn't simply miss a discharge location? This "false negative" risk is exacerbated by the heterogeneity of natural geologic materials and human emplaced materials at industrial sites. Such complex, mixed subsurface structures typically include preferential flow pathways, so discharge can be highly localized and occur in a small percentage of the total area of a site. It is typically not feasible to verify that every potential flow path has been identified. Non-destructive characterisation *via* geophysical methods can be informative, but are often inconclusive due to the complexity of the subsurface materials and barriers to signal penetration.

Therefore, the delineation of groundwater discharge from sediment often must utilize direct measurement at the sediment–surface water interface. Here we expand on recent advancements (*e.g.*, (ref. 2, 7, 8, 11 and 13)), to provide a statistically-sound and pragmatic implementation of the fiber optic based method that can be used in many settings to achieve direct detection of groundwater discharges. Unlike point measurement methods, this approach offers more complete site coverage and high-resolution data, offering greater

[a]*SelkerMetrics, Portland, OR, USA*
[b]*EA Engineering Science and Technology, Hunt Valley, MD, USA*
[c]*ExxonMobil Environmental Services Company, Houston, TX, USA*

confidence that the largest seeps have been located. The suggested methods are demonstrated at site-scale.

Groundwater temperature is generally quite stable, while surface water temperatures change seasonally and daily. For this reason, at certain times of year seeps may be detected by looking for temperature anomalies at the sediment interface. Remote sensing of temperature signatures of seepage has been studied using infrared imagery (*e.g.*, (ref. 1)). While sometimes informative, the fact that infrared imagery is only sensitive to the temperature of the water at the air interface precludes seep detection of low mass-flux discharge in water of significant depth, in water bodies with significant mixing due to flow, or in waters that are thermally stratified. Furthermore, infrared imagery, like spot sampling and many other methods, provides only a snap-shot at one point in time. However, many important discharge systems are episodic, driven by tides and recharge events such as rainfall that may frustrate one-time methods.

Recent environmental applications have suggested that distributed temperature sensing (DTS) can provide thermal detection of areas of discharge along long transects and with high spatial resolution.[2–5,7,11,13] In brief, DTS uses a fiber optic cable to detect temperature differences as small as 0.02 °C along cables that are multiple kilometers in length, and with sub-meter spatial resolution. In essence, DTS offers a practical way to collect temperature data continuously from thousands of precise and durable thermometers at or below the sediment–water interface.

We will refer to the application of DTS to identification of discharge as DTSID. This can be implemented by crisscrossing an area of interest with fiber optics to identify thermal anomalies that may indicate possible discharges. We present a methodology for the design, installation, and interpretation of data from DTSID to identify and prioritize sampling locations for characterization of possible groundwater discharges. A stochastic layout method offers a pre-determined probability of detection for a specified size, shape, and orientation of seep. We demonstrate results from three industrial sites.

Equipment and methods

Heat has been used as an indicator of water movement in hydrologic systems, particularly in tracing groundwater seeps.[6–8] The technique has increased in utility as the temporal and spatial resolution of temperature measurement has improved: spatial range has been extended to many kilometers, and temperature measurements have become more accurate and precise. While DTS was developed over 20 years ago,[9,10] it is only since 2006 and as the systems' performance has improved that this method has been applied in hydrology.[2,6–8,11–13]

DTS temperature measurements are obtained from a fiber optic based on the ratio of amplitudes of two of the colors of light that are scattered within the fiber. These signals are the result of the Raman effect, in which a fraction of incident laser light interacts inelastically with the electrons in the molecular bonds of the glass (described in detail in 2 and 4). Following absorption by a glass molecule of a photon from the injected light, the glass molecule emits a photon with frequency either below (Stokes) or above (anti-Stokes) that of the injected light, reflecting the quantum energy states of the particular electron which the photon encountered. The higher the temperature is the greater the number of electrons in high-energy states, increasing the ratio of anti-Stokes scattering relative to the Stokes signal. The ratio of these signals provides a measure of fiber temperature. The location of the backscatter is determined by the elapsed time between pulse injection and observation of the backscattered light. Since only an infinitesimal fraction of the incident light is scattered in an optical fiber, backscatter signal intensities are low. This, together with the stochastic distribution of photon energies, is the primary limit on the precision of DTS measurement. Greater temperature precision may be achieved by longer integration time (waiting for more backscattered light – the standard deviation of measurement declines with the square root of duration), brighter lasers (more photons per unit time), and more sensitive detectors (greater fraction of returning photons detected). Greater spatial resolution requires more precise measurement of the timing of backscatter and reduces the number of photons per unit length of fiber. Thus there are trade-offs between precision of temperature, duration of measurement, and spatial resolution. In this application, rapid measurements are generally not required, but the trade-off between spatial resolution (detecting smaller features) and precision (detect smaller changes) is relevant.

The length of fiber is primarily limited by the loss of light that occurs with increased distance of travel. Longer cables also require greater time between laser pulses to avoid overlapping returned light, reducing data collection per unit of time. For this application, cable lengths have typically been in the range of two to five kilometers.

The DTS used for this study was the Sensornet Oryx, with minimum sample spacing of 1 m. Because temperatures reported for 1 m segments are affected by adjacent segments, the spatial resolution (*i.e.*, distance between essentially statistically independent readings) is 2 m. Instruments are now available with 0.125 m sampling and 0.3 m resolution, providing finer detail and the potential detection of smaller seeps.

Under laboratory conditions, the cable and DTS allows distinguishing temperature variations along the cable as small as 0.01 °C,[2] while in field conditions, integrating over several hours, this value is typically 0.02–0.03 °C for this instrument with the use of continuous re-calibration. There are typically additional uncertainties regarding absolute temperature (accuracy), but these are not critical for this application because we only require relative differences along the cable, rather than absolute temperatures.

The detection of seepage using temperature requires a detectable contrast in temperature between surface water and the source of seepage. In general, groundwater systems have a stable temperature near the annual average air temperature. The greatest contrast in temperature is typically obtained when the surface water is either at its warmest during late summer or at its coldest in late winter. The temperature contrast available

for detection is also affected by thermal stratification in surface waters, particularly in the summer.

The installation of the fiber optic cable greatly affects the sensitivity of the measurement. In general the cable should be denser than water and sediment, so that it will sink into soft sediment or rest firmly on a firm sediment interface. Typical muds have densities below 2000 kg m^{-3}, so cables should be selected with density of at least 3000 kg m^{-3}, with greater density being advantageous. Durable cables that protect the fiber from damage are helpful in this application. In the work described here we employ a cable (BruMarine, Brugg Cables, Switzerland) with a diameter of 10 mm consisting of a polyethylene jacket surrounding an 8 mm core built up of helically wrapped steel wires. Two 1.1 mm stainless steel tubes were incorporated, each containing one graded index, multi-mode fiber. The complete cable had a density of 3400 kg m^{-3}.

In environments having little or no current, sediment interfaces are typically soft, and dense cables will sink below the interface surface without additional effort. The cable being below the sediment interface increases the sensitivity of the method.[14] In higher energy environments, observation of seeps is complicated both by the greater difficulty in positioning the cable below the typically harder sediment interface and the dissipation of seepage thermal effects by water movement. Tests with a flume designed to emulate field conditions, with controlled seep rates and currents, have confirmed findings from the case studies presented here, showing that the combination of cable placement, substrate texture, and current velocity affect the sensitivity and feasibility of temperature-based seep detection (data not shown).

In the studies presented here, the DTS cable was paid from a motorized spool positioned on the shore, floated using removable foam blocks to a GPS-positioned boat. The cable was secured in place with anchors (typically 5 kg boat anchors). Anchor locations were confirmed by GPS after placement. Key considerations in cable laying include avoiding kinking or bending that can damage the fiber optic, safety of deployment, and an installation that is compatible with waterway usage. In some cases it has been helpful to use divers for cable placement, embedding the cable in sediment and documenting as-built cable location, but in other installations divers are not required. A weather station was installed in order to correlate findings with precipitation, temperature, solar heating, wind speed and other weather impacts. In marine environments, tides and salinity were also monitored which were helpful in the interpretation of temperature dynamics, as will be shown.

The spacing of DTSID cable and spatial resolution along the cable determine the likelihood of intercepting seeps of various sizes. Thus the minimum size of a seep that is acceptable to miss helps determine the spacing of the DTSID cable layout. There is a probabilistic element to detection of seeps that are below certain sizes: seeps that are large relative to the system resolution are certain to overlap a cable, and thus be detected, but small seeps may sometimes overlap a cable and may sometimes fall between cables.

To date there has been no literature addressing systematic design of a DTSID layout to address this. To estimate the probabilities of seep detection of a given DTSID layout, we address the stochastic nature of seepage through used of a Monte Carlo simulation. This simulation places tens of thousands of hypothetical seeps on a site with a DTSID layout that is being considered. Seeps are modeled as ellipses drawn randomly from specified distributions of size, location, orientation, and elongation. By tabulating whether each seep sufficiently overlaps the fiber optic cable to be detected (based on DTS performance specifications), the simulation provides an estimate of the probability of detecting seeps as a function of size and characteristics. Orientation was specified as preferentially occurring in the direction of site stratigraphy. This simulation helps select among preferred orientations of the DTSID, as well as the required density of the layout.

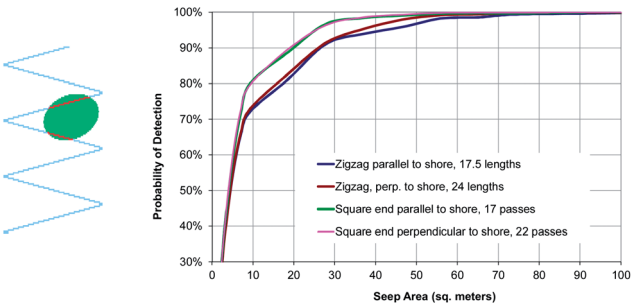

Fig. 1 Illustrations of a stochastic DTSID layout simulation. At left a stochastically generated elliptical seep is superimposed on zig-zag pattern cable layout. Red cable segments showing overlap of the cable and a seep. Chart shows probabilities of detecting seeps of various sizes for four alternative layouts. In this example, square-ended layouts (where cables run parallel rather than in a triangular patter as shown to the left) offered higher probabilities of detection of intermediate-sized seeps, while number of cable passes had little effect.

An example of the results of 50 000 trials for a particular layout and set of seep assumptions is shown in Fig. 1. One could further define a probability of detection for seeps overlaying the cables as a function of the length of cable which intersects the seeps, seep flux rate or volume, burial depth, currents, or other characteristics that may affect detection.

Analysis

Temperature differences associated with seeps can be limited due to low flux rates, surface water movement, modest temperature differential between surface and groundwater, and conduction of heat from the surface water into the sediments. Adding to the challenge, there can be significant temperature variations in the surface water through diurnal cycles, tides, and changing weather. Analysis, visualization, and signal processing methods were used to isolate the signal of interest. Varying conditions at different installations required differing analyses and visualizations, and multiple methods and lines of evidence were considered.

Because of the intrinsic uncertainties in seepage detection, we consider the DTSID method suitable for prioritizing locations for follow-up sampling to verify the existence and absence of seeps. At some sites DTSID can provide direct evidence for

the existence of seeps, for example, by showing tidal temperature fluctuations suggestive of seeps. At other sites, DTSID cannot prove or rule out seeps, but allows prioritizing areas of a site for likelihood of seepage. If follow up investigation finds that seeps are not present, even in areas with relatively strong DTSID indications, the likelihood of seeps at any locations on the site is low. DTSID does not offer certainty for all sites, but with results corroborated using sampling and other means, the DTSID's high-resolution view over a large area allows extending or extrapolating those findings to an entire site and can offer increased confidence that significant seeps have not been missed.

Because the DTSID system records over 100 000 temperatures per kilometer of cable per day, an installation typically creates data sets of millions of values. This offers opportunities for statistical analysis that are not feasible with many other environmental monitoring methods. We assumed that temperature distributions are approximately normal and applied a one-sided *t*-test comparing temperatures of a given area with other temperature measurements within a surrounding area. By varying the spatial sizes of the respective areas and the magnitude of the specified temperature difference taken to be indicative of seepage, one can identify and prioritize regional thermal anomalies. We also calculated standard deviations of temperature over time to identify areas that had less temperature variability, perhaps due to groundwater seeps of constant temperature.

The large data sets also support creating animation videos that show changes over time and can be helpful for seeing patterns of temperature variability and persistence of cool or warm temperatures.

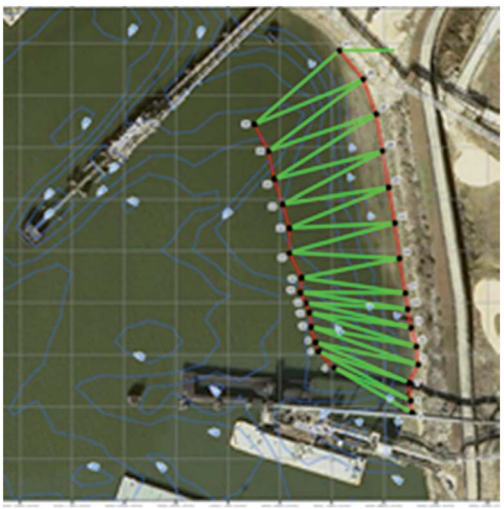

Fig. 2 DTSID zigzag cable (green) deployment on a sloping marine shore near an industrial site in Texas. Layout designed to identify seeps of greater than 2800 m^2 with over 99% probability.

Case studies

We consider three case studies which illustrate several characteristic features of the DTSID method. In the first study, a direct analysis of measured temperatures enabled identifying likely seeps. In the second case, systematic patterns of thermal fluctuations in time and space were removed to obtain seepage signals that could be interpreted. Finally, a site with strong tidal influence provides evidence that temperature variability indeed reflects seepage. The variety of layout geometries among sites reflect in part differences in currents, sediment type, and depth, that affect the practicality of alternative deployment and anchoring approaches.

The first site experiences modest tides and was monitored during June, when groundwater temperatures averaged 7 °C cooler than surface waters (Fig. 2). Emerging groundwater was

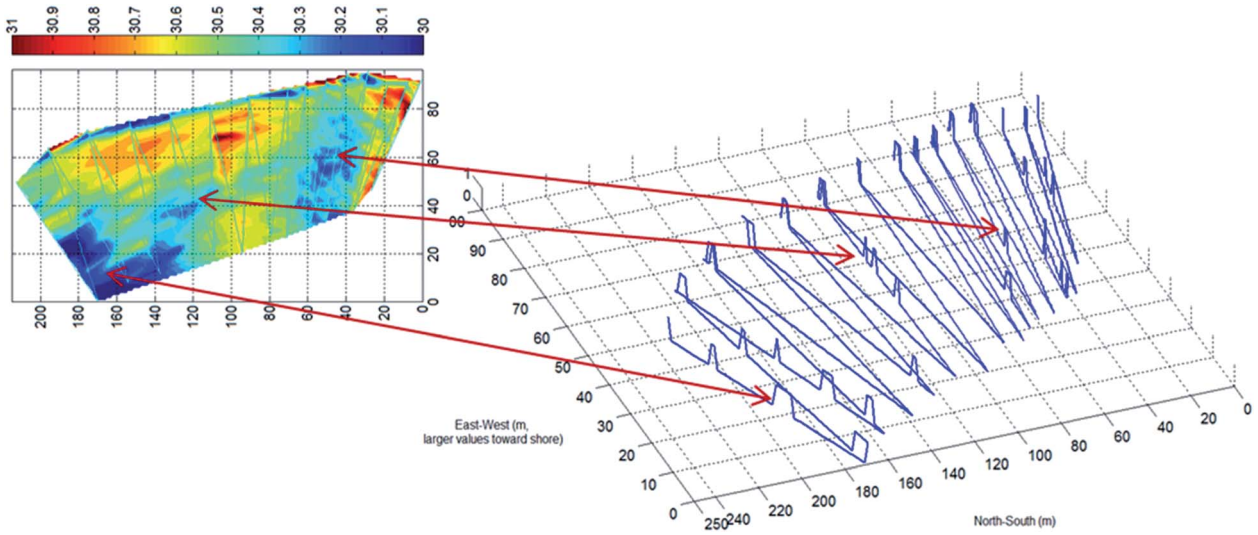

Fig. 3 Contour plot shows average temperature (°C) measured on bay bottom for June 12–30, 2009 at site shown in Fig. 2. Interpolation between data points in the contour plot was done with the MatLab griddata function. Cool (blue) areas may indicate areas with cool groundwater seepage. Near-shore temperatures (top) are distorted by exposure during low tides. Line plot on right shows locations that are statistically cooler as raised (*z*-axis value 1, rather than zero), with correspondence to cool areas highlighted by connecting red arrows.

neutral to slightly buoyant relative to the saline surface water. The layout was simulated and the northern portion of the layout was found to have a 70% probability of intercepting a seep with area 50 m^2, a 97% probability of detecting a seep of 300 m^2, and over 99% probability of intercepting a seep of 2800 m^2. The southern portion of the site had tighter spacing of cable, so detection probabilities would exceed these values.

By taking the multi-day averages of DTSID data, variations associated with weather and tidal influence were removed to leave average temperatures (color contour image, left in Fig. 3). Shoreline temperatures (strip along the top) were affected by exposure during low tides and could not be used. Blue areas reflect cool sediment that could indicate seepage.

Locations found to be statistically significantly cooler than those in their immediate vicinity are shown with correspondence (red arrows) to the average temperatures across the site (peaks on right hand side of Fig. 3, indicate locations that are at least 0.15 °C warmer than surrounding areas 2–7 m away, $p < 0.001$, one-sided t-test). Areas with the bulk of statistically cooler locations, indicated by multiple peaks, correspond to areas that are, on average, cooler, which is expected for areas affected by seeps.

During summer installations such as this one, the stratification of water temperature can be a confounding factor since deeper water is typically cooler than surface water. Tides can exacerbate the impact of stratification, since thermoclines sweep up and down across the area of interest and expose areas to sun and warm air temperatures. However, an analysis of temperature and temperature variability *versus* depth revealed locations that were cooler and less variable than typical locations of the same depth (Fig. 4). Certain depths had an over-representation of such points, suggesting the possibility of stratigraphic reasons for groundwater emergence at these depths.

A second installation was in a shallow tidally-effected inlet at an industrial site in Texas (Fig. 5). The pond has roughly

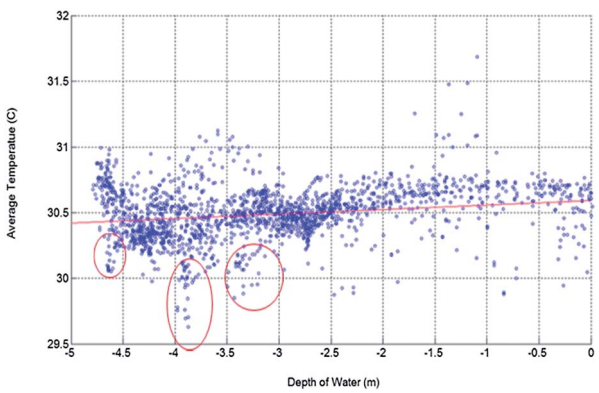

Fig. 4 Average summer temperature *vs.* depth at sloped site. Temperature shows gradual decline with depth, with the average temperature falling about 0.3 °C at about 1.5 m down to a depth of 4.75 m. Minimum average temperatures occur not at the deepest locations, but at about 3.5–4.5 meters in depth. Ovals highlight groups of locations with low temperature, and there are also low-temperature points scattered in shallower water consistent with seepage.

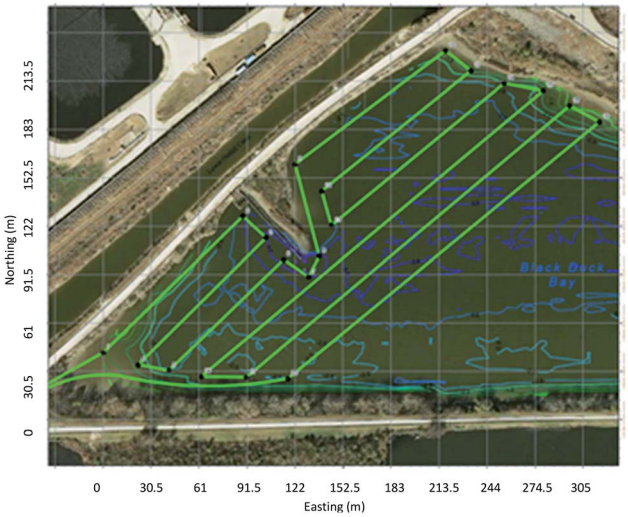

Fig. 5 Shallow (<2 m) pond with DTSID cable location shown (bright green). The pond is connected to a marine bay, so the water level fluctuates with area tides. Irregular lines show bathymetry, with depth varying by about 0.5 m across the installation.

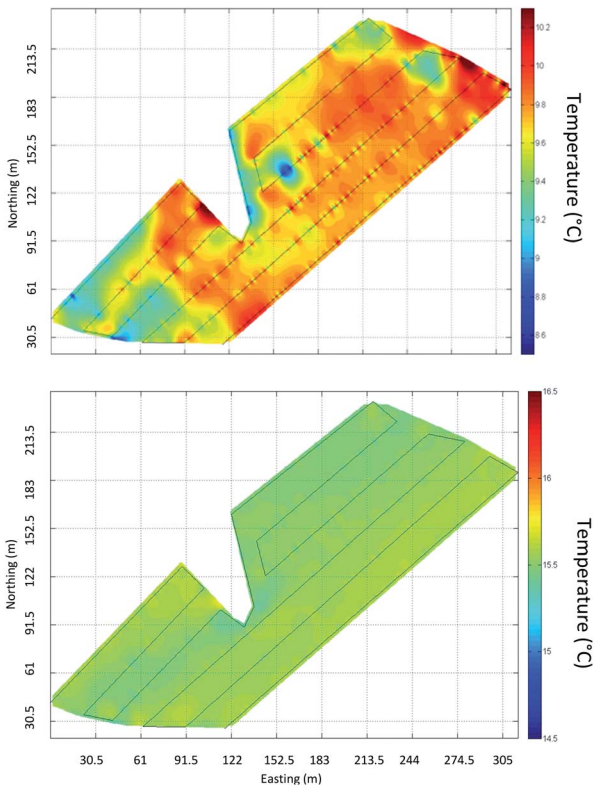

Fig. 6 Temperature during low tide (upper image) shows variability. Because monitoring was done during winter when groundwater was warmer than surface water, warm areas (red) are likeliest seepage locations. During high tide (lower image) temperatures are nearly uniform perhaps due to the increased hydrostatic pressure of higher water levels halting or reversing groundwater flow into the bay. Interpolation between data points in the contour plot was done with the MatLab griddata function.

uniform depth and no currents. Data was collected during January and February, when groundwater averaged 11 °C warmer than surface water. This pond is connected to a tidally affected canal, so the water level fluctuates with area tides. The layout was simulated and found to have a 95% probability of detecting a seep of 280 m^2 and over 99% probability of detecting a seep of 2800 m^2.

Fig. 6 shows this location at low tide (top image) and high tide (lower image), respectively. During low tides the temperature variability on the pond sediment is over three times greater than the variability during high tides. We believe the variability during low tides reflects variability caused by varying seep rates, with red (warm) areas being highest priority for seep investigation. During high tides, it appears seeps reverse, with surface water intruding into sediment and eliminating temperature variation. In this case an animation of temperature variability also showed this temperature variability changing with tide level. This illustrates a benefit of dynamic monitoring through time, since seeps can be affected by changing conditions such as tides, precipitation, or remedial action such as pumping or barriers.

A third, larger DTSID study was carried out along the shore of a marine bay in Western Canada, with data analyzed in both summer and winter. Winter temperatures showed less variability due to: (1) reduced diurnal temperature swings; (2) reduced thermal stratification; (3) reduced solar heating since winter low tides occurred at night; and (4) air temperatures that were similar to water temperatures. Winter weekly variations in mean cable temperature were about 2–5 °C *versus* 10–20 °C in summer. Beyond these winter advantages which will exist at most sites, at this location the summer deep water remained cool even as the surface warmed, yielding little distinction between groundwater and bay water temperature. In winter the groundwater was about 7 °C warmer than surface water, providing the contrast needed for DTSID monitoring. Thus analysis was conducted using data from two winter seasons. The eastern third of the installation was simulated and found to have a 60% probability of detecting a 5 m^2 seep, an 80% probability for a 10 m^2 seep, an 87% probability for a 20 m^2 seep, and 97% for a 30 m^2 seep. The remaining areas utilized similar cable spacing.

Where feasible, the cable was embedded about 4 cm into the fine sand and sediment. This was accomplished by divers in the deeper sections of cable and from the shore in the large intertidal zone. Some sections of cable could not be embedded and were held off the sediment by rocks or debris, and no such sections of cable held above the sediment showed results indicative of possible seeps. Tidal currents and convection are expected to mix seeping groundwater sufficiently that a cable held away from the surface is unlikely to detect seep temperature effects, and this was borne out at this site.

Temperature differences of less than one tenth of a degree can be of interest in identification of potential seeps. However, thermoclines and tidal exposure created unrelated variations ranging from about one (winter) to two (summer) orders of magnitude larger than such anticipated seep signals. Two

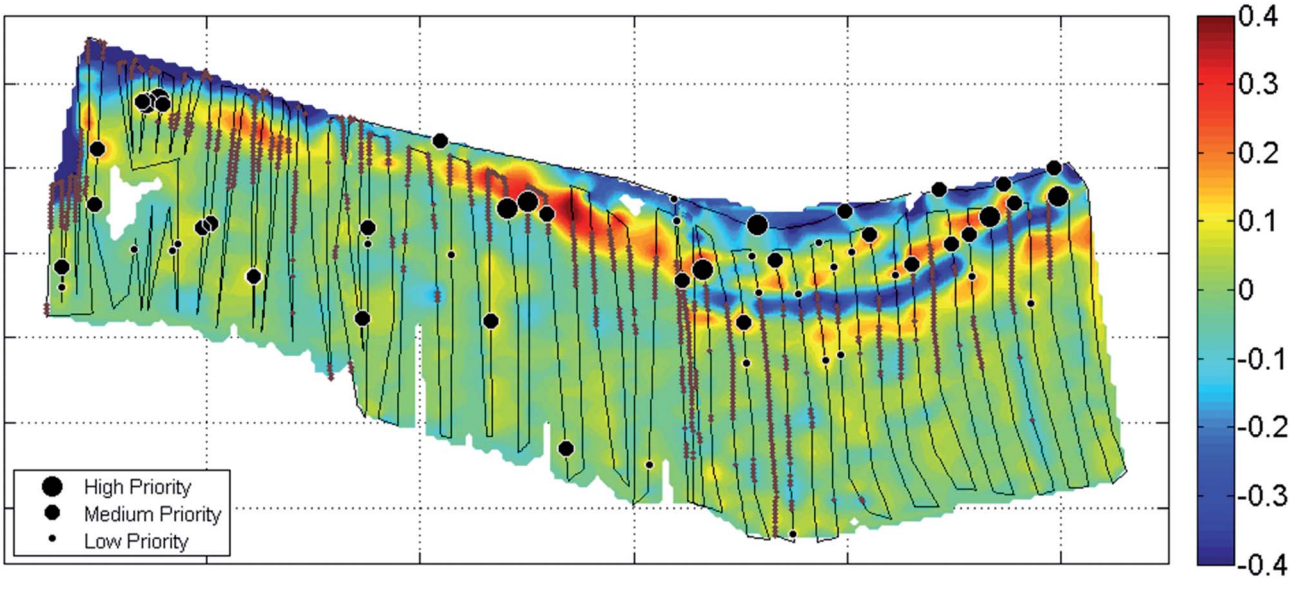

Fig. 7 Prioritizations of temperature anomalies summarized for potential follow-up sampling. Priority, shown by circle size, reflects the size of the temperature anomaly, the breadth of the area involved, statistical analysis, and the goal of sampling several areas with anomalies. Color represents mean fiber temperatures minus the average surrounding temperature in a 20 m diameter. Groundwater was warmer than surface water during winter, so seeps would be expected to be warm. Data for the center and western installations are from winter 2012–2013; eastern installation data are from winter 2011–2012. Eastern data are from low tides when contrast was greatest, other areas average all tides since contrast did not vary by tide. The three installations each covered about one third of the area shown. Small brown beads along the cable indicate sections which were not embedded in sediment. 6 km of total cable installation, total area 2.3 hectares. Some of the warm (red) areas near shore were not prioritized because cable position did not allow good data collection (*e.g.*, over rocks), statistical analysis did not indicate a seep, and/or detailed examination of temperature fluctuations did not indicate anomalies suggesting seeps.

methods were used to model and remove temperature variations associated with thermoclines and tides. In the first method, each location along the fiber optic cable was compared with other locations located at similar elevation and/or showing similar mean temperatures during high tides, when cable is fully submerged and seeps are expected to be reversed or at low flows. Residual temperature differences, which were found to be robust relative to noise cancelling parameters, were then used to seek possible seeps. In the second (Fig. 7) the average temperature of an area surrounding each point was subtracted from the point temperature. Thus, if the point was unusually warm, the residual temperature was positive and if it were the same or cooler than neighboring points, it would be zero or negative. This is analogous to how statistical testing was calculated and provided excellent enhancement power in the identification of unusual locations.

A number of near-shore areas were identified as priorities for follow up to investigate the possibility of seepage occurring. The scarcity of signs of seepage in deeper locations is consistent with fresh groundwater rising to the top of the contact with denser saline water, expected to result in groundwater emergence near the surface of the saltwater at the shore. Seeps that were visible during low tide were detected by the DTSID method and identified as priorities at the northeastern corner of the site (Fig. 7).

Conclusions

DTSID allows continuous collection of precise temperatures over extended times and large areas of sediment. This enables identifying and prioritizing locations as having possible groundwater discharges and monitoring changes with tides, weather, remedial actions, and other factors. A stochastic approach to designing the DTSID layout facilitated achieving desired detection probabilities for seeps of specified sizes while accounting for DTS performance and expected seep orientation based on local geology. Case studies demonstrate the capability of the method at locations that are most likely to either have discharges or an absence of such discharges. Limitations to DTSID include challenges discerning seep-related temperature effects among other sources of temperature fluctuations; that the method is not yet able to quantify flux rates; and the attenuation of signal with currents and placement on rocks that prevent contact with sediment. For these reasons, DTSID should generally be a part of an integrated site investigation that includes follow up seep testing with other methods and/or sampling.

Burial offers a stronger temperature signal than surface placement and mitigates impacts of currents. DTSID has also been used to detect inflows to small streams, an application for which currents do not pose a problem and for which burial is not necessary.

At many sites DTSID offers a practical and effective way to identify locations with the highest likelihood of groundwater emerging into sediments and surface waters. It offers a line of evidence with the advantages of high-resolution, testing over large areas, and providing a continuous and dynamic view of potential seeps.

Acknowledgements

Research funded by ExxonMobil and Imperial Oil. We acknowledge the field assistance of staff of CH2MHill in Houston and Golder and Associates in Western Canada.

Notes and references

1 S. P. Loheide and S. M. Gorelick, *Environ. Sci. Technol.*, 2006, **40**, 3336–3341.
2 J. S. Selker, L. Thévenaz, H. Huwald, A. Mallet, W. Luxemburg, N. Van de Giesen, M. Stejskal, J. Zeman, M. Westhoff and M. B. Parlange, *Water Resour. Res.*, 2006, **42**, W12202.
3 L. D. Slater, D. Ntarlagiannis, F. D. Day-Lewis, K. Mwakanyamale, R. Versteeg, A. Ward, C. Strickland, C. D. Johnson and J. W. Lane, *Water Resour. Res.*, 2010, **46**, W10533, DOI: 10.1029/2010wr009110.
4 S. W. Tyler, J. S. Selker, M. B. Hausner, C. E. Hatch, T. Torgersen, C. E. Thodal and G. Schladow, *Water Resour. Res.*, 2009, DOI: 10.1029/2008wr007052.
5 M. B. Hausner, F. Suárez, K. E. Glander, N. Giesen, J. S. Selker and S. W. Tyler, *Sensors*, 2011, **11**, 10859–10879.
6 K. B. Moffett, S. W. Tyler, T. Torgersen, M. Menon, J. S. Selker and S. M. Gorelick, *Environ. Sci. Technol.*, 2008, **42**, 671–676.
7 O. A. C. Hoes, W. M. J. Luxemburg, M. C. Westhoff, N. van de Giesen and J. S. Selker, *Lowland Technology International*, 2009, **11**, 21–26.
8 R. D. Henderson, F. D. Day-Lewis and C. F. Harvey, *Geophys. Res. Lett.*, 2009, **36**, L06403.
9 J. P. Dakin, D. J. Pratt, G. W. Bibby and J. N. Ross, *Electron. Lett.*, 1985, **21**(13), 569–570.
10 T. Kurashima, T. Horiguchi and M. Tateda, *Opt. Lett.*, 1990, **15**(18), 1038–1040.
11 J. S. Selker, N. van de Giesen, M. Westhoff, W. Luxemburg and M. B. Parlange, *Geophys. Res. Lett.*, 2006, **33**, 24401, DOI: 10.1029/2006gl027979.
12 M. C. Westhoff, H. H. G. Savenije, W. M. J. Luxemburg, G. S. Stelling, N. van de Giesen, J. S. Selker, L. Pfister and S. A. Uhlenbrook, *Hydrol. Earth Syst. Sci.*, 2007, **11**, 1469.
13 C. S. Lowry, J. F. Walker, R. J. Hunt and M. P. Anderson, *Water Resour. Res.*, 2007, **43**, 10408.
14 S. Krause, T. Blume and N. J. Cassidy, *Hydrol. Earth Syst. Sci.*, 2012, **9**, 337–378.

